


Article

Antiproliferative and Antimigration Activities of Beauvericin Isolated from *Isaria* sp. on Pancreatic Cancer Cells

Hiroaki Yahagi, Tadahiro Yahagi , Megumi Furukawa and Keiichi Matsuzaki *

School of Pharmacy, Nihon University, 7-7-1 Narashinodai, Funabashi, Chiba 274-8555, Japan; phhi17001@g.nihon-u.ac.jp (H.Y.); yahagi.tadahiro@nihon-u.ac.jp (T.Y.); manyu0907@hotmail.com (M.F.)

* Correspondence: matsuzaki.keiichi@nihon-u.ac.jp; Tel.: +81-47-465-5356

Received: 15 September 2020; Accepted: 5 October 2020; Published: 8 October 2020



Abstract: This study describes the antiproliferative and antimigration effects of beauvericin from a culture broth of *Isaria* sp. in human pancreatic cancer cells (PANC-1). Activity-guided fractionation of the EtOAc extract of cultured broth of *Isaria* sp. RD055140 afforded beauvericin (**1**), a new isariotin derivative, 7-*O*-methylisariotin C (**2**), together with the known isariotin analogs, TK-57-164A (**3**) and B (**4**). As a result of the measurement of the cell viability, **1** inhibited cell growth ($IC_{50} = 4.8 \mu M$) of PANC-1 cells. Furthermore, **1** was found to inhibit the migration activity of PANC-1 cells by upregulating the expression of the *E-cadherin* gene and reducing *N-cadherin* and *Snail* genes in a dose-dependent manner (0.1–1 μM). These activities of **1** had lower concentrations than the cytotoxic activity. These findings suggest that **1** can be used as an anticancer agent against human pancreatic carcinoma.

Keywords: beauvericin; EMT; entomopathogenic fungi; *Isaria*; isariotin; migration; pancreatic cancer

1. Introduction

Pancreatic cancer is one of the most common tumors worldwide, but its malignancy leads to poor prognosis. Basal treatment is surgical resection, but it is difficult to find in early stages due to few subjective symptoms and the ease of distant metastasis. As a result, it can be managed with this treatment only in limited cases [1,2]. Because the majority of cases are found in advanced stages, this cancer responds poorly to currently available medical therapies. Hence, it is necessary to develop novel anticancer agents to inhibit cancer proliferation or metastasis.

Some reports suggest that epithelial to mesenchymal transition (EMT) plays an important role in tumor progression and metastasis, including pancreatic cancer. EMT occurs by loss of epithelial cells and acquisition of mesenchymal characteristics by stimulation of some factors, such as transforming growth factor (TGF- β), fibroblast growth factor (FGF) and hypoxia-inducible factor (HIF), and so on. During EMT progression, the expression of epithelial markers, e.g., *E-cadherin*, *occludin* or *cytokeratin*, is downregulated, while mesenchymal markers, such as *N-cadherin*, *vimentin* and *fibronectin* are upregulated. Moreover, transcriptional factors, such as *Snail*, *Slug*, *Zeb-1*, and *Twist1*, are associated with the regulation of the expression of these markers, so it is important to control such factors to suppress the EMT process of pancreatic cancer [3,4].

Entomopathogenic fungi are parasitic to some species of insects. These fungi kill the host insect to acquire nutrients and grow into a fruiting body. They are used as a portion of healthy food and traditional medicine in Asian countries. They produce various secondary metabolites with a wide variety of biological activities, such as anticancer [5], immunosuppressant and cardiovascular [6].

We hypothesize that compounds that have an inhibitory activity on cell growth and EMT could be candidates for anticancer drugs against pancreatic cancers, which have cells that can easily acquire

abilities of migration and invasion. Based on a cytotoxicity screening of pancreatic cancer cell lines, the EtOAc extract of *Isaria* sp. RD055140 showed strong inhibitory activity. In this report, for the isolation of active compounds from *Isaria* sp. and the evaluation of the activity (cell viability: 31.4%, 10 $\mu\text{g/mL}$, positive control: cisplatin, 69.2%, 100 μM), we describe the structural analysis of four compounds and the assessment of their active mechanisms toward EMT.

2. Results

2.1. Structures of 1–4

The EtOAc extract of *Isaria* sp. RD055140 exhibiting inhibitory activity of cell growth was fractionated on bioassay-guided fractionation to afford 1–4 (Figure 1).

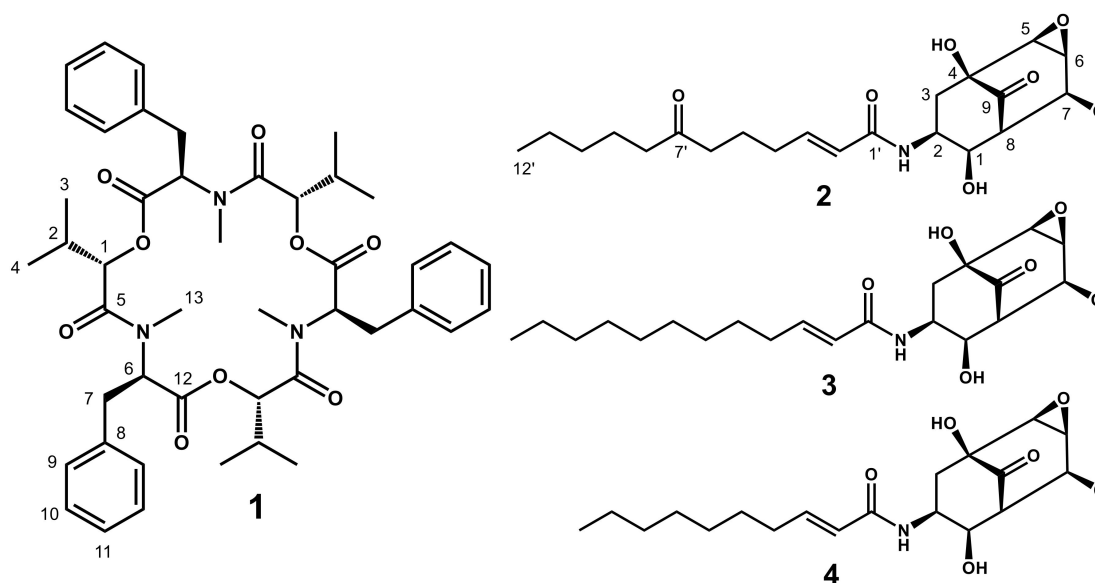


Figure 1. Structures of isolated compounds from the EtOAc extract of the culture medium of *Isaria* sp. RD055140.

Compound 1 was identified as beauvericin by comparison of its NMR and MS spectra with those reported [7].

Compound 2 was obtained as a colorless amorphous solid and had $[\alpha]_{25\text{D}} -46.5$ (c 0.10, CH_3OH). The molecular formula of 1 was determined to be $\text{C}_{22}\text{H}_{33}\text{NO}_7$ by HR-ESI-MS (m/z 446.2155 $[\text{M} + \text{Na}]^+$, calcd. for 446.2155), corresponding to 8 degrees of unsaturation. IR absorption bands suggested an amino functional group at 3390 cm^{-1} , hydroxyl functional groups at 3298 cm^{-1} , amide and keto carbonyls at $1748, 1708, 1674, 1635\text{ cm}^{-1}$ and an ether functional group at 1082 cm^{-1} . The $^1\text{H-NMR}$ spectrum displayed one methyl proton signal at $\delta_{\text{H}} 0.90$ (t, $J = 7.0\text{ Hz}$), seven methylenes at $\delta_{\text{H}} 1.27$ (m), $\delta_{\text{H}} 1.32$ (m), $\delta_{\text{H}} 1.55$ (m), $\delta_{\text{H}} 1.71$ (m), $\delta_{\text{H}} 2.19$ (q, $J = 7.0\text{ Hz}$), $\delta_{\text{H}} 2.44$ (t, $J = 7.0\text{ Hz}$), $\delta_{\text{H}} 2.49$ (t, $J = 7.5$), one methine at $\delta_{\text{H}} 3.05$ (ddd, $J = 1.0, 3.5, 7.5$), two olefins at $\delta_{\text{H}} 6.01$ (d, $J = 15.5\text{ Hz}$) and another at $\delta_{\text{H}} 6.78$ (m), one methoxy at $\delta_{\text{H}} 3.48$ (s), four oxymethines at $\delta_{\text{H}} 3.49$ (dd, $J = 1.5, 3.5\text{ Hz}$), $\delta_{\text{H}} 3.48$ (s), $\delta_{\text{H}} 3.88$ (d, $J = 7.5\text{ Hz}$) and $\delta_{\text{H}} 4.30$ (q, $J = 2.0\text{ Hz}$) and one *N*-methine at $\delta_{\text{H}} 4.73$ (dq, $J = 2.5, 13.0\text{ Hz}$). The $^{13}\text{C-NMR}$, DEPT, and HMQC spectra showed 22 carbon signals, which could be assigned one methyl signal at $\delta_{\text{C}} 14.28$, eight methylenes at $\delta_{\text{C}} 23.37$, $\delta_{\text{C}} 23.52$, $\delta_{\text{C}} 24.57$, $\delta_{\text{C}} 32.26$, $\delta_{\text{C}} 32.52$, $\delta_{\text{C}} 38.59$, $\delta_{\text{C}} 42.49$, $\delta_{\text{C}} 43.52$, one methine at $\delta_{\text{C}} 57.25$, two olefinic methines at $\delta_{\text{C}} 125.06$ and another at $\delta_{\text{C}} 145.39$, four oxygenated methines at $\delta_{\text{C}} 65.16$, $\delta_{\text{C}} 56.46$, $\delta_{\text{C}} 72.04$, $\delta_{\text{C}} 78.71$, one *N*-methine at $\delta_{\text{C}} 47.67$, one oxygenated quaternary carbon at $\delta_{\text{C}} 77.25$, two keto carbonyls at $\delta_{\text{C}} 208.77$ and another at $\delta_{\text{C}} 213.56$, one amide at $\delta_{\text{C}} 167.78$ and one methoxy at $\delta_{\text{C}} 58.64$. The HMBC spectrum revealed that proton signals at $\delta_{\text{H}} 2.09$ (t, $J = 13.0\text{ Hz}$, H-3b) and $\delta_{\text{H}} 2.24$ (ddd, $J = 1.5, 5.0, 13.0\text{ Hz}$, H-3a) both correlated to the

methylene at δ_C 38.59 (C-2), which indicated these proton signals were non-equivalent. The ^1H - ^1H COSY spectrum clarified the hydrogen sequence in bold, as shown in Figure 2. The interrelationships of these partial structures were determined by HMBC experiment. The HMBC correlations from proton signals at δ_H 4.30 (H-1) to carbon signals δ_C 208.77 (C-9), from δ_H 2.24 and δ_H 2.09 (H-3) to δ_C 77.25 (C-4) and C-9, from δ_H 3.49 (H-5) to C-9, from δ_H 3.88 (H-7) to δ_C 56.46 (C-6) and C-5 and from δ_H 3.05 (H-8) to C-6 and C-9 indicated that this molecule had the bicyclo[3.3.1]nonane carbon skeletal structure (C-1–C-9). The ^1H -NMR spectrum also revealed mutually coupled signals at H-5 and H-6, which correlated to the methine carbon signals at C-5 and C-6, respectively, in the HMQC spectrum. The chemical shifts of these signals showed the presence of an epoxide functional group in this molecule. Other HMBC cross-peaks from δ_H 6.01 (H-2') to δ_C 167.78 (C-1'), from δ_H 2.49 (H-6') to δ_C 213.56 (C-7') and from δ_H 2.44 (H-8') to δ_C 213.56 (C-7') indicated this molecule had a side chain composed of 12 carbons. The side chain was located at C-2 by HMBC correlation from H-2 to amide carbonyl at C-1'. The HMBC correlation between H-7 and the methoxy carbon at δ_C 58.64 indicated the location of a methoxy group at C-7. As a result of these spectral analyses, the structure of **2** was proposed as 7-O-methylisariotin C, which is a new compound.

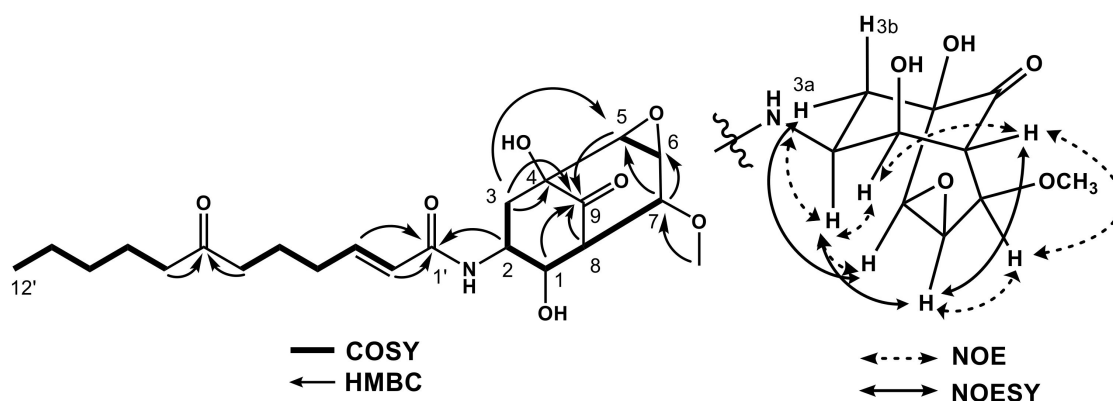


Figure 2. Key correlations of 2D NMR and relative configuration for **2**.

Compounds **3** (TK-57-164A) and **4** (TK-57-164B) were found to be constitutional isomers of **2** when the NMR and MS spectra were compared with those previously reported [8,9].

2.2. Measurement of Cell Viability

To evaluate the potential effect of **1–4** on human pancreatic cancer cellular proliferation, we used the human pancreatic cancer cell line PANC-1. An MTT proliferation assay demonstrated that **2–4** did not show an inhibitory effect on cell growth, but **1** decreased the viability of PANC-1 at the concentration of 1–10 μM (IC_{50} = 4.8 μM) in a dose-dependent manner (Figure 3).

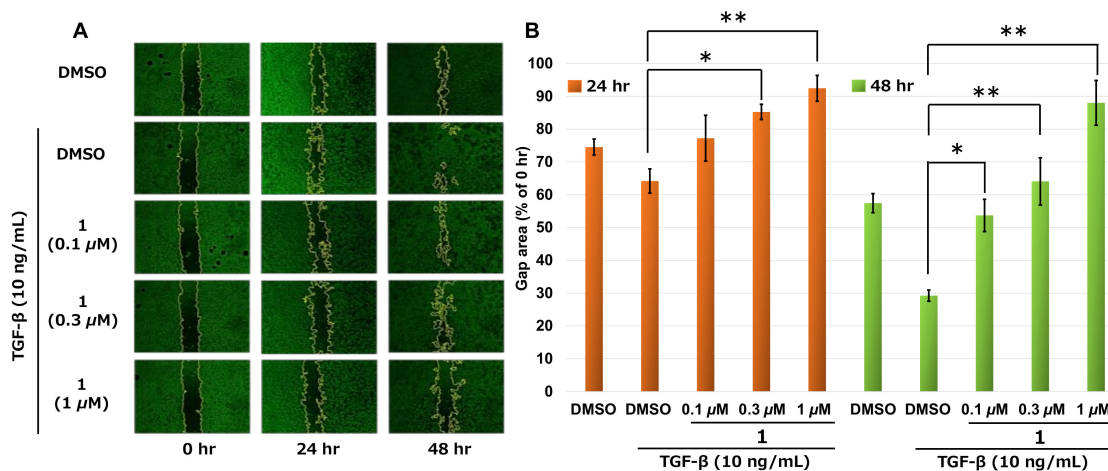


Figure 3. Effect of **1** on the migration of PANC-1 cells. (A) Wound-healing assay, PANC-1 cells grown at confluency. The monolayers were scratched with a 200 μL pipette tip in the central area of the culture. TGF- β and **1** were added at the indicated times. Photographs were taken using phase-contrast microscopy (magnification at 40 \times). (B) Quantification of the cell-free area. Quantification was done using NIH Image J (ver. 1.51). Statistical analysis was performed using JMP 14. Data are expressed as the mean \pm SE. These experiments were done in triplicate (N = 3). * $p < 0.05$, ** $p < 0.01$.

2.3. Measurement of Cell Migration by Wound-Healing Assay

We performed a wound-healing assay to evaluate whether **1** can inhibit not only cell viability, but also the cell migration of PANC-1. After 48 h of incubation with 10 ng/mL TGF- β and 0.1–1 μM of **1**, the motility of PANC-1 cells was inhibited, whereas the cells treated with 10 ng/mL TGF- β and vehicle DMSO migrated through the wounded area to close the wound (Figure 3). Furthermore, we investigated the effect of **1** on the expression of EMT marker genes in PANC-1 cells in the presence of TGF- β . In Figure 4, cells treated with 10 ng/mL TGF- β for 48 h. led to an increase in the mRNA of EMT markers such as *N-cadherin*, *Snail*, and *Slug* and a decrease in *E-cadherin*, so TGF- β induced EMT by signal transduction in PANC-1 cells. Furthermore, cells treated with TGF- β plus 1 μM of **1** upregulated the expression of *E-cadherin* and decreased that of *N-cadherin* and *Snail*.

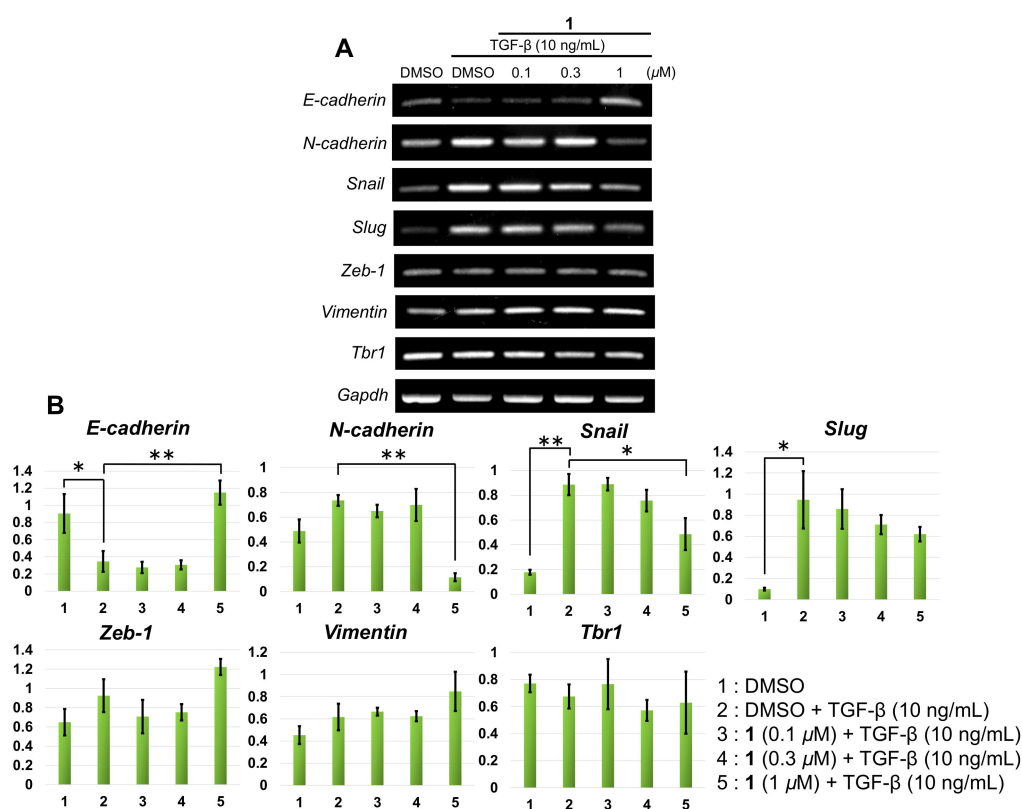


Figure 4. Compound 1 inhibited epithelial to mesenchymal transition (EMT) by regulating the expression of EMT markers. (A) The expression of mesenchymal markers of EMT in the mRNA level was measured by RT-PCR. PANC-1 cells were treated with TGF-β and 1 (0.1–1 μM) for 48 h. (B) Quantification of each marker. Quantification was done using NIH Image J (ver. 1.51). Statistical analysis was performed using JMP 14. Data are expressed as the mean ± SE from independent experiments. * $p < 0.05$, ** $p < 0.01$.

3. Discussion

The present study elucidates the effects of four compounds isolated from *Isaria* sp. RD055140 for cytotoxicity and migration and the mechanisms of migration activity on cells of the pancreatic cancer cell line PANC-1. Beauvericin (1), but not isariotin analogs (2–4), showed significant antiproliferative activity. In addition, 1 inhibited cell migration in a dose-dependent manner by the mechanisms of upregulation of *E-cadherin* and downregulation of *N-cadherin* and *Snail* genes.

EMT occurs frequently in the progression of various malignancies like migration and invasion [10]. As TGF-β is released from the marginal cells of tumor cells, it is associated with this process and enhances the activity of migration [11]. The regulation of the TGF-β signal pathway is effective in inhibiting cancer progression. We evaluated the effect of 1 treatment on the migration ability using a wound-healing assay to find that 0.1–1 μM of 1 significantly inhibited migration of PANC-1 cells with a lower dose of cytotoxic activity ($IC_{50} = 4.8 \mu\text{M}$). Our results (Figure 3) showed 1 had the ability of antagonistic activity toward TGF-β signaling. However, the underlying mechanisms at this point are unclear, and further studies are needed to clarify this.

It is known that TGF-β signaling downregulates *E-cadherin*, *occludin* and *cytokeratin*, while upregulates *N-cadherin*, *vimentin*, *fibronectin*, *Snail*, *Slug*, *Zeb-1* and *Twist1* to progress EMT [11]. This results in a loss of epithelial phenotypes and the acquisition of mesenchymal phenotypes and leads to EMT. Consequently, regulating these factors is an important key to inhibiting tumor progression, so we evaluated the effect of 1 for EMT-related factors by RT-PCR. Our results showed that 1 inhibited the downregulation of *E-cadherin* and the upregulation of *N-cadherin* and *Snail* genes, while little

influenced *Zeb-1*, *Vimentin* and *Tbr1*. These results indicate that **1** could regulate not only epithelial but also mesenchymal genes.

Beauvericin is a cyclic hexadepsipeptide that belongs to the enniatin family produced by various fungi and has many biologic activities, especially anticancer effects [12]. Beauvericin has been reported to induce the apoptosis of human non-small cell lung cancer cells and human epidermoid carcinoma cells through mitochondrial pathways, including the decrease of reactive oxygen species, loss of mitochondrial membrane potential, the release of cytochrome c and activation of caspase-9 and -3 [13,14]. Many reports have been published about its anticancer effects, including apoptosis and oxidative stress in vitro. However, studies focusing on the inhibition of cell migration have not been reported [7], and this mechanism has not been examined. Based on our research, this study is the first report that describes not only cytotoxicity but also the antimigration activity and the mechanisms of the inhibitory effect of beauvericin on EMT via the TGF- β -signaling pathway on PANC-1 pancreatic cancer cells. Both beauvericin and enniatins have antibiotic and ionophoric properties and different bioactivities [15]. Reports that enniatin affects cell migration have not been published. Therefore, it is necessary to further investigate the structure-activity relationship between beauvericin and similar compounds and the further precise mechanisms underlying the inhibitory effect on EMT.

Isariotins were originally isolated from the cultured broth of *I. tenuipes*, and many derivatives have been isolated from *Isaria* species [16]. Because some isariotin analogs have been reported to exhibit cytotoxic activities against human epidermoid carcinoma cells, small cell lung cancer cells and human breast cancer cells [17,18], they are considered as the candidates for novel anticancer agents. We isolated three isariotin analogs, including one new compound in this report, but unfortunately, they have no effects against the viability of PANC-1 cells. Thus, we hope to investigate isariotin derivatives, which have inhibitory activities on cell growth and cell migration on PANC-1 cells.

In conclusion, this study has demonstrated for the first time that **1** inhibits TGF- β -induced EMT by regulating EMT-related genes in pancreatic cancer. Because of the difficulty of early detection, pancreatic cancer is often considered one of the poorest-prognosis cancers compared to any other cancer type. Many patients need to take an anticancer agent, for example, gemcitabine, 5-FU, cisplatin or paclitaxel; however, these drugs are not effective enough [11]. Resolving this problem is a key factor in improving the prognosis of pancreatic cancer. As such, our research provides a possible lead to the development of a new anticancer agent that has both inhibitory activities of cell growth and EMT.

4. Materials and Methods

4.1. General Procedures

UV and IR spectra were recorded using a V-730 BIO spectrophotometer and an FT/IR-4200 spectrophotometer (JASCO, Tokyo, Japan), respectively. Optical rotations were determined using a P1020 polarimeter (JASCO, Tokyo, Japan). NMR spectra were measured using a JNM ECX-500 NMR and JNM ECX-600 NMR spectrometer (JEOL, Tokyo, Japan). ESI mass spectra were obtained using a Xevo G2-S QTOF (Waters, Milford, MA, USA).

Dimethyl sulfoxide (DMSO), 10 \times phosphate-buffered saline (PBS) and agar were purchased from FUJIFILM Wako Pure Chemical Corporation (Osaka, Japan). 3-[4,5-Dimethylthiazol-2-yl]-2,5-diphenyl-tetrazolium (MTT) was purchased from Dojindo Molecular Technologies, Inc. (Kumamoto, Japan). Methanol- d_4 was purchased from Kanto Chemical Co., Inc. (Tokyo, Japan). Cisplatin was purchased from Sigma-Aldrich Co. LLC (St. Louis, MO, USA). TGF- β was purchased from BioLegend, Inc. (San Diego, CA, USA). Roswell Park Memorial Institute media (RPMI 1640) was purchased from Nacalai Tesque (Kyoto, Japan). Fetal bovine serum and penicillin-streptomycin were purchased from Gibco (Grand Island, NY, USA). DifcoTM potato dextrose broth (PDB) and DifcoTM potato dextrose agar (PDA) were purchased from Becton, Dickinson and Company (Franklin Lakes, NJ, USA).

4.2. Cell Culture

PANC-1, a human pancreatic cancer cell line, was purchased from RIKEN BioResource Research Center (Ibaraki, Japan) and was cultured in RPMI 1640 supplemented with 10% FBS and 1% penicillin-streptomycin at 37 °C in an atmosphere of 5% CO₂.

4.3. Measurement of Cell Viability by MTT Assay

PANC-1 cells were plated on a 96-well plate at 1×10^5 cells/mL and incubated. After 24 h, the medium was changed and treated with various concentrations of the samples. Control cells were treated with DMSO. After incubation of the cells with samples for 48 h, 20 µL of 1 mg/mL MTT solution was added to each well and incubated at 37 °C for four hours. The supernatant was then removed and 150 µL DMSO was added to each well to dissolve the formazan. The formazan formation was measured with a microplate reader at a wavelength of 570 nm and a reference wavelength of 655 nm.

4.4. Extraction and Isolation of Chemical Compounds from *Isaria* sp. RD055140

Isaria sp. RD055140 that was purchased from the National Institute of Technology and Evaluation (NITE) Biological Resource Center (NBRC) was precultured in a PDA medium for seven days in a 10 cm Petri dish. Cultured agar medium was hollowed out by a cork borer (7 mm i.d.), inoculated in 300 mL or 500 mL baffled Erlenmeyer flasks containing 100 mL or 150 mL of PDB medium and cultured for seven days at 25 °C on a rotary shaker at 150 rpm.

The cultured broth (10.5 L) was extracted with the same volume of EtOAc and filtered. The EtOAc layer was concentrated in vacuo to give the EtOAc extract (1.14 g). The extract was chromatographed on preparative silica gel TLCs developed with CHCl₃-CH₃OH-H₂O (90:12:1), and each fraction was extracted with CH₃OH (250 mL) to obtain 10 fractions (fr. 1 to 10). The third fraction (202.5 mg) was purified by HPLC (column: YMC Pack Pro C18 (10 mm i.d. × 250 mm), flow-rate: 3.0 mL/min) using a gradient program of CH₃OH-H₂O (7:3)/0 min → (9:1)/60 min as an eluate to give **1** (22.2 mg). The fourth fraction was purified on HPLC using the same column, eluted with a gradient of CH₃OH-H₂O (6:4)/0 min → (9:1)/60 min and yield **2** (3.5 mg), **3** (5.6 mg) and **4** (5.6 mg).

Beauvericin (**1**): colorless amorphous solid, $[\alpha]_{25D} +6.14$ (c 0.1, CH₃OH); HR-ESI-MS m/z [M + Na]⁺ 806.3987 (calcd. for C₄₅H₅₇N₃O₉Na, 806.3990); ¹H- and ¹³C-NMR (600 MHz, 150 MHz, CD₃OD): See Table S1.

7-O-methylisariotin C (**2**): colorless amorphous solid, $[\alpha]_{25D} -46.5$ (c 0.1, CH₃OH); HR-ESI-MS m/z [M + Na]⁺ 446.2155 (calcd. for C₂₂H₃₃NO₇Na, 446.2155); UV λ_{max} (CH₃OH, log ϵ) 208 nm (4.25), FT-IR (KBr) 3390, 3289, 2939, 1748, 1708, 1674, 1635, 1082 cm⁻¹; ¹H- and ¹³C-NMR (500 MHz, 125 MHz, CD₃OD): See Table S2.

TK-57-164A (**3**): colorless amorphous solid, $[\alpha]_{25D} -7.57$ (c 0.1, CH₃OH); HR-ESI-MS m/z [M + Na]⁺ 432.2361 (calcd. for C₂₂H₃₅NO₆Na, 432.2362); ¹H- and ¹³C-NMR (500 MHz, 125 MHz, CD₃OD): See Table S2.

TK-57-164B (**4**): colorless amorphous solid, $[\alpha]_{25D} -6.90$ (c 0.1, CH₃OH); HR-ESI-MS m/z [M + Na]⁺ 404.2053 (calcd. for C₂₀H₃₁NO₆Na, 404.2049); ¹H- and ¹³C-NMR (500 MHz, 125 MHz, CD₃OD): See Table S2.

4.4.1. Measurement of Cell Migration by Wound-Healing Assay

PANC-1 cells were seeded in 24-well plates at 2×10^5 cells/mL and cultured for 48 h until they reached confluence. Then, a linear wound was generated in the monolayer with a sterile 200 µL micropipette tip. Any cellular debris was removed twice with PBS and incubated with serum-free RPMI 1640 medium with samples together with 10 ng/mL TGF- β . Control cells were treated with DMSO and with or without TGF- β . After incubation for 24 and 48 h, the cells were photographed with a digital camera, and the migrated area was measured using NIH Image J (ver. 1.51) software.

4.4.2. Reverse Transcription-Polymerase Chain Reaction (RT-PCR)

The expression levels of *E-cadherin*, *N-cadherin*, *Snail*, *Slug*, *Zeb-1*, *Vimentin* and TGF- β receptor 1 (*Tbr1*) mRNA were determined using RT-PCR. After incubation on a 24-well plate in a sample-containing medium for 48 h, total RNAs were extracted using an RNeasy Mini Kit (Qiagen, Hilden, Germany), following the manufacturer's instructions. Reverse transcription reactions were performed with a PrimeScript RT-PCR Kit (Takara Bio, Inc., Shiga, Japan) following the manufacturer's instructions, using 250 ng of total RNA. The expression levels of the above genes were confirmed using *Gapdh* as a control.

The primers had the following sequences: for *E-cadherin*, forward: 5'-GCCTCCTGAAAA GAGAGTGGAAAG-3', reverse: 5'-TGGCAGTGTCTCTCCAAATCCG-3', for *N-cadherin*, forward: 5'-GAGGAGTCAGTGAAGGAGTCA-3', reverse: 5'-GGCAAGTTGATTGGAGGGATG-3', for *Snail*, forward: 5'-TGCCCTCAAGATGCACATCCGA-3', reverse: 5'-GGGACAGGAGAAGGGCTTCTC-3', for *Slug*, forward: 5'-ATCTGCGGCAAGGCGTTTTCCA-3', reverse: 5'-GAGCCCTCAGATTTGACC TGTC-3', for *Slug*, forward: 5'-ATCTGCGGCAAGGCGTTTTCCA-3', reverse: 5'-GAGCCCTCAG ATTTGACCTGTC-3', for *Zeb-1*, forward: 5'-AAGTAACCCTGTGTATTTCTGGATGA-3', reverse: 5'-TGGGATCAACCACCAATGG-3', for *Vimentin*, forward: 5'-AGGCAAAGCAGGAGTCCACTGA-3', reverse: 5'-ATCTGGCGTTCCAGGGACTCAT-3', for *Tbr1*, forward: 5'-CGCACTGTCATTCACCAT-3', reverse: 5'-AAACCTGAGCC AGAACCT-3' and for *Gapdh*, forward: 5'-ACGGATTTGGTCGT ATTGGG-3', reverse: 5'-TGATTTTGGAGGGATCTCGC-3'.

4.5. Statistical Analysis

The data are expressed as the means \pm standard error (SE). Quantification was done using NIH Image J ver. 1.51 (National Institutes of Health, Rockville, Maryland, USA). Statistical comparisons among different treatment groups were performed using one-way analysis of variance (ANOVA) with Dunnett's multiple comparison test using JMP 14 (SAS Institute Inc., Cary, NC, USA). The level of statistical significance was set at $p < 0.05$ or 0.01.

Supplementary Materials: The following are available online, Figure S1: ^1H -NMR spectrum of **1** in CD_3OD , Figure S2: ^{13}C -NMR spectrum of **1** in CD_3OD , Figure S3: COSY spectrum of **1** in CD_3OD , Figure S4: HMQC spectrum of **1** in CD_3OD , Figure S5: HMBC spectrum of **1** in CD_3OD , Figure S6: NOE spectra of **1** in CD_3OD (1), Figure S7: NOESY spectrum of **1** in CD_3OD (2).

Author Contributions: Conceptualization, H.Y. and K.M.; validation, M.F. and T.Y.; formal analysis, H.Y.; investigation, H.Y.; resources, T.Y.; data curation, K.M.; writing—original draft preparation, H.Y.; writing—review and editing, K.M.; visualization, T.Y.; supervision, K.M.; project administration, K.M.; funding acquisition, K.M. All authors have read and agreed to the published version of the manuscript.

Funding: This work was supported in part by the "Private University Research Branding Project" from MEXT (2018) and Nihon University Chairman of the Board of Trustees Grant (2019–2020).

Acknowledgments: We are indebted to Dr. Koichi Metori of the Analytical Center of the School of Pharmacy, Nihon University, for the measurements of the mass spectra.

Conflicts of Interest: The authors declare no conflict of interest.

References

1. Siegel, R.L.; Miller, K.D.; Jemal, A. Cancer statistics CA. *Cancer. J. Clin.* **2018**, *68*, 7–30. [[CrossRef](#)] [[PubMed](#)]
2. Saung, M.T.; Zheng, L. Current standards of chemotherapy for pancreatic cancer. *Clin. Ther.* **2017**, *39*, 2125–2134. [[CrossRef](#)] [[PubMed](#)]
3. Gonzalez, D.M.; Medici, D. Signaling mechanisms of the epithelial-mesenchymal transition. *Sci Signal.* **2014**, *7*, re8. [[CrossRef](#)] [[PubMed](#)]
4. Gaianigo, N.; Melisi, D.; Carbone, C. EMT and treatment resistance in pancreatic cancer. *Cancers* **2017**, *9*, 122. [[CrossRef](#)] [[PubMed](#)]
5. Yue, K.; Ye, M.; Zhou, Z.; Sun, W.; Lin, X. The genus *Cordyceps*: A chemical and pharmacological review. *J. Pharm. Pharmacol.* **2013**, *65*, 474–493. [[CrossRef](#)] [[PubMed](#)]

6. Fujita, T.; Hirose, R.; Yoneta, M.; Sasaki, S.; Inoue, K.; Kikuchi, M.; Hirase, S.; Chiba, K.; Sakamoto, H.; Arita, M. Potent Immunosuppressants, 2-Alkyl-2-aminopropane-1,3-diols. *J. Med. Chem.* **1996**, *39*, 4451–4459. [[CrossRef](#)] [[PubMed](#)]
7. Zhan, J.; Burns, A.M.; Liu, M.X.; Faeth, S.H.; Gunatilaka, A.A.L. Search for cell motility and angiogenesis inhibitors with potential anticancer activity: Beauvericin and other constituents of two endophytic strains of *Fusarium oxysporum*. *J. Nat. Prod.* **2007**, *70*, 227–232. [[CrossRef](#)] [[PubMed](#)]
8. Nakagawa, A.; Nishikawa, N.; Takahashi, S.; Yamamoto, K. Substances TK-57-164A and TK-57-164B, process for producing the same and agricultural/horticultural bactericides containing the same. J. P. Patent WO-A1-2004/074269, 2004.
9. Asai, T.; Chung, Y.M.; Sakurai, H.; Ozeki, T.; Chang, F.R.; Wu, Y.C.; Yamashita, K.; Oshima, Y. Highly oxidized ergosterols and isariotins analogs from an entomopathogenic fungus, *Gibellula formosana*, cultivated in the presence of epigenetic modifying agents. *Tetrahedron* **2012**, *68*, 5817–5823. [[CrossRef](#)]
10. Bozzuto, G.; Ruggieri, P.; Molinari, A. Molecular aspects of tumor cell migration and invasion. *Ann. Ist. Super. Sanita.* **2010**, *46*, 66–80. [[CrossRef](#)] [[PubMed](#)]
11. Xu, J.; Lamouille, S.; Derynck, R. TGF- β -induced epithelial to mesenchymal transition. *Cell Res.* **2009**, *19*, 156–172. [[CrossRef](#)] [[PubMed](#)]
12. Wu, Q.; Patocka, J.; Nepovimova, E.; Kuca, K. A review on the synthesis and bioactivity aspects of beauvericin, a *Fusarium* mycotoxin. *Front. Pharmacol.* **2018**, *9*. [[CrossRef](#)] [[PubMed](#)]
13. Lin, H.I.; Lee, Y.J.; Chen, B.F.; Tsai, M.C.; Lu, J.L.; Chou, C.J.; Jow, G.M. Involvement of Bcl-2 family, cytochrome c and caspase 3 in induction of apoptosis by beauvericin human non-small cell lung cancer cells. *Cancer Lett.* **2005**, *230*, 248–259. [[CrossRef](#)] [[PubMed](#)]
14. Tao, Y.W.; Lin, Y.C.; She, Z.G.; Lin, M.T.; Chen, P.X.; Zhang, J.Y. Anticancer activity and mechanism investigation of beauvericin isolated from secondary metabolites of the mangrove endophytic fungi. *Anticancer Agents Med. Chem.* **2015**, *15*, 258–266. [[CrossRef](#)] [[PubMed](#)]
15. Liuzzi, V.C.; Mirabelli, V.; Cimmarusti, M.T.; Haidukowski, M.; Leslie, J.F.; Logrieco, A.F.; Caliandro, R.; Fanelli, F.; Mulè, G. Enniatin and beauvericin biosynthesis in *Fusarium* species: Production profiles and structural determinant prediction. *Toxins* **2017**, *9*. [[CrossRef](#)] [[PubMed](#)]
16. Zhang, X.; Hu, Q.; Weng, Q. Secondary metabolites (SMs) of *Isaria cicadae* and *Isaria tenuipes*. *RSC Adv.* **2019**, *1*, 172–184. [[CrossRef](#)]
17. Bunyapaiboonsri, T.; Yoiprommarat, S.; Intereya, K.; Rachtawee, P.; Hywel-Jones, N.L.; Isaka, M. Isariotins E and F, spirocyclic and bicyclic hemiacetals from the entomopathogenic fungus *Isaria tenuipes* BCC12625. *J. Nat. Prod.* **2009**, *72*, 756–759. [[CrossRef](#)] [[PubMed](#)]
18. Bunyapaiboonsri, T.; Yoiprommarat, S.; Srisanoh, U.; Choowong, W.; Tسانathai, K.; Hywel-Jones, N.L.; Luangsa-ard, J.J.; Isaka, M. Isariotins G–J from cultures of the *Lepidoptera* pathogenic fungus *Isaria tenuipes*. *Phytochem. Lett.* **2011**, *4*, 283–286. [[CrossRef](#)]

Sample Availability: Samples of the compounds are not available from the authors.



© 2020 by the authors. Licensee MDPI, Basel, Switzerland. This article is an open access article distributed under the terms and conditions of the Creative Commons Attribution (CC BY) license (<http://creativecommons.org/licenses/by/4.0/>).